Brazilian Journal
of Chemical
Engineering

ISSN 0104-6632
Printed in Brazil
www.abeq.org.br/bjche

Vol. 26, No. 01, pp. 45 - 52, January - March, 2009

BOUNDARY LAYER THICKNESS OF CYLINDERS AND PLANE SURFACES IMMERSED IN PACKED BEDS IN ALIGNMENT WITH THE FLOW

J. M. P. Q. Delgado

Departamento de Engenharia Química , Faculdade de Engenharia da Universidade do Porto,
Fax: + (351) 225081449, Rua Dr. Roberto Frias, s/n, 4200-465, Porto, Portugal.
E-mail: jdelgado@fe.up.pt

(Submitted: June 14, 2007 ; Revised: August 14, 2008 ; Accepted: August 30, 2008)

Abstract - In this work, boundary layer development was investigated for a mass transfer process between a moving fluid and a slightly soluble cylinder or plane surface buried in a packed bed, in alignment with the direction of flow. The bed of inert particles is taken to have uniform voidage. For this purpose, numerical solutions of the partial differential equations describing mass concentration of the solute were undertaken to obtain the concentration boundary layer thickness as a function of the relevant parameters. Mathematical expressions that relate the dependence with the Peclet number and aspect ratio of the immersed active surfaces are proposed to describe the approximate size of the concentration boundary layer thickness.
Keywords: Concentration boundary layer; Molecular diffusion; Packed bed; Soluble cylinder; Flat wall; High-resolution schemes.

INTRODUCTION

There are several situations of practical interest, both in nature and in man-made processes, in which a solid cylinder or plane surface immersed in a packed bed of small inert particles interacts with the fluid flowing around it, through the interstices in the bed.

Flows along buried cylindrical or flat surfaces (a particular case of a cylindrical surface with "infinite" radius) are important model situations and, in the present work, are investigated numerically for very wide ranges of values of Peclet number, Pe', and aspect ratio of the immersed surfaces.

Prandtl (1910) introduced the concept of a boundary layer for fluid flow past a solid in the early years of the last century. Over the years, several analytical steady and unsteady state mass transfer solutions for concentration boundary layer thickness, δ, have been presented in the literature (Schlichting, 1979) for the case of a thin boundary layer (high Peclet numbers). Curiously, the lack of correlations for concentration boundary layer thickness of cylinders and plane surfaces buried in porous media and in alignment with the flow, at low fluid velocities, motivated this work.

The influence of the rheological properties on the boundary layer thickness was studied in detail by different scientists. For example, Nebbali and Bouhadef (2006) showed that, when the permeability and/or kinematic viscosity is increased, the velocity gradients at the duct walls decrease, which results in a boundary layer thickness increase. Cheng (2007) showed that increasing the power-law index or decreasing the Lewis number or decreasing the buoyancy ratio tends to increase the fluid velocity, which results in a concentration boundary layer thickness increase.

In this paper, numerical relationships for the concentration boundary layer thickness applicable to dissolving cylindrical or flat surfaces under steady-state conditions are obtained, for the whole range of relevant parameters.

*To whom correspondence should be addressed

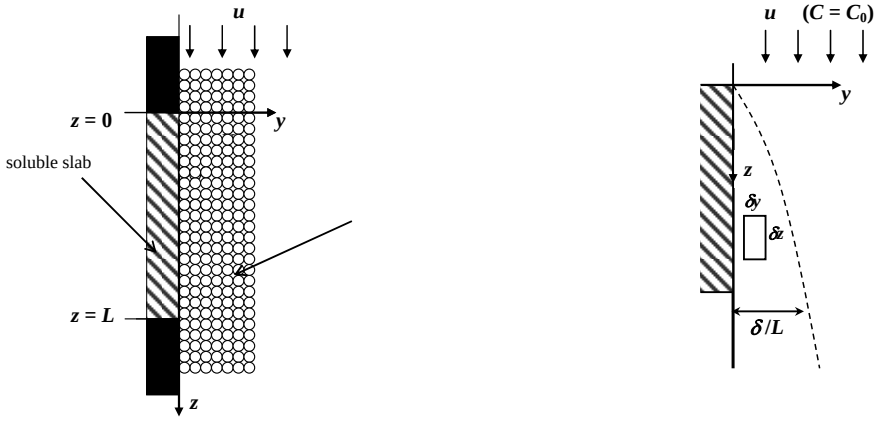

Figure 1: (a) – Flow along soluble slab; (b) – Mass transfer boundary layer

THEORY

Case I - Soluble Flat Slab

Figure 1 sketches a section through a packed bed along which liquid is flowing, close to a flat wall, part of which (0< z< L) is slightly soluble. Liquid flow will be taken to be steady, with uniform average superficial velocity u, and, if the concentration of solute in the liquid fed to the bed is c_0 and the solubility of the solid wall is c*, a mass transfer boundary layer will develop, across which the solute concentration drops from c=c*, at y=0, to $c \rightarrow c_0$, for large y. The main assumptions are: steady-state, constant velocity, and the medium is treated as a continuum and isotropic medium.

It is well known (e.g., Vortmeyer and Schuster, 1983) that the voidage of a packed bed (and therefore the fluid velocity) is higher near a containing flat wall, but in the case of our study it may be considered that such a non-uniformity will have negligible effect. For one thing, if we consider that the bed particles have diameters between 0.2 and 0.5 mm, consequently the region of increased voidage will be very thin. Furthermore, because the inert particles making up the bed indent the soluble surface slightly as dissolution takes place, there is in fact virtually no near wall region of higher voidage.

If we restrict our analysis to those situations for which the mass transfer boundary layer extends over several particle diameters and if a small control volume is considered, inside this boundary layer, with side lengths δz, δy and unity (perpendicular to the plane of the figure), a steady state material balance for the solute leads to:

$$u\frac{\partial c}{\partial z} = D_T\frac{\partial^2 c}{\partial y^2} + D_L\frac{\partial^2 c}{\partial z^2} \tag{1}$$

where D_T and D_L are the dispersion coefficients, respectively, in the cross-stream and in the stream-wise directions. If the boundary layer is thin compared to the length of the soluble slab, the last term on the r.h.s. of (1) will be negligible (see Coelho and Guedes de Carvalho, 1988 for a quantitative treatment of this aspect) and Eq. (1) then reduces to the equation of diffusion in one dimension to be solved with:

$$c = c_0 \qquad z = 0 \qquad y > 0 \tag{2a}$$

$$c = c^* \qquad z > 0 \qquad y = 0 \tag{2b}$$

$$c \rightarrow c_0 \qquad z > 0 \qquad y \rightarrow +\infty \tag{2c}$$

The solution is the well-known complementary function error:

$$\frac{c - c_0}{c^* - c_0} = \operatorname{erfc}\left(\frac{y}{2}\sqrt{\frac{u}{D_T z}}\right) \tag{3}$$

The concentration boundary layer thickness is defined as the vertical distance from the cylindrical or flat surfaces where the solute concentration is 1%

of the saturation concentration. For the case of $D_L \cong D_T \cong D'_m$ and for a laminar boundary layer with a conservative dissolving flat plane, the analytical solution (3) can be written (see Chrysikopoulos et al., 2003) as:

$$\delta \cong 2\sqrt{\pi}\left(\frac{D'_m z}{u}\right)^{0.5} \tag{4}$$

valid when the superficial velocities are very high.

Here we wish to consider the mass transfer process for the whole range of superficial velocities, so the term accounting for longitudinal dispersion will have to be considered and Eq. (1) will have to be integrated numerically. In order to integrate Eq. (1), it is convenient to define the following dimensionless variables:

$$C = \frac{c - c_0}{c^* - c_0} \tag{5a}$$

$$Y = \frac{y}{L} \tag{5b}$$

$$Z = \frac{z}{L} \tag{5c}$$

$$Pe' = \frac{uL}{D'_m} \tag{5d}$$

where Pe' represents the Peclet number (based on the length, L, of the soluble slab), and D'_m is the effective molecular diffusion coefficient, defined as the ratio between the molecular diffusion coefficient and the tortuosity, τ, of the packed bed ($D'_m = D_m / \tau$).

In terms of dimensionless variables, Eq. (1) for $D_L \cong D_T \cong D'_m$ (isotropic porous bed), may then be rewritten as:

$$Pe'\frac{\partial C}{\partial Z} = \frac{\partial^2 C}{\partial Z^2} + \frac{\partial^2 C}{\partial Y^2} \tag{6}$$

and the appropriate boundary conditions are:

$$C \to 0 \qquad Z \to -\infty \qquad \forall Y \tag{7a}$$

$$C = 1 \qquad 0 \le Z \le 1 \qquad Y = 0 \tag{7b}$$

$$\frac{\partial C}{\partial Y} = 0 \qquad Z < 0 \vee Z > 1 \qquad Y = 0 \tag{7c}$$

$$C \to 0 \qquad \forall Z \qquad Y \to +\infty \tag{7d}$$

$$C \to 0 \qquad Z \to +\infty \qquad Y \ge 0 \tag{7e}$$

Equation (6) is to be solved numerically, subject to the boundary conditions (7a-e), over a large range of Pe' values.

Case II - Cylinder Aligned with the Flow

Another important situation, sketched in Figure 2, is a slightly soluble cylinder of diameter $d_1 (= 2a)$ and length L buried in a packed bed of inert particles with uniform porosity, along which fluid flows with uniform superficial velocity, u. A mass transfer boundary layer develops, across which the concentration of solute drops from $c = c^*$, at $r = a$, to $c \to c_0$, for large enough r.

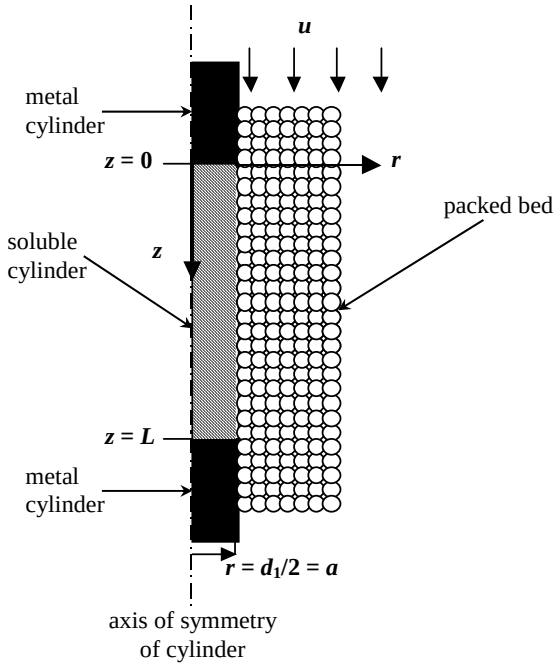

Figure 2: along soluble cylinder.

Taking a radial co-ordinate, r, to measure distance to the axis of the buried cylinder and a co-ordinate z, to measure distance along the average flow direction, the differential mass balance for the solute reads:

$$\frac{D_T}{r}\frac{\partial}{\partial r}\left(r\frac{\partial C}{\partial r}\right) + D_L\frac{\partial^2 C}{\partial z^2} = u\frac{\partial C}{\partial z} \tag{8}$$

In order to solve Eq. (8) numerically, with $D_L \cong D_T \cong D'_m$, it is convenient to use the dimensionless variables represented by Eqs. (7a), (7c), (7d) and $R = r / a$. Eq. (8) may then be rewritten as:

$$Pe'\frac{\partial C}{\partial Z}=\frac{\partial^2 C}{\partial Z^2}+4\left(\frac{L}{d_1}\right)^2\frac{1}{R}\frac{\partial}{\partial R}\left(R\frac{\partial C}{\partial R}\right) \qquad (9)$$

and the appropriate boundary conditions are:

$$C\to 0 \qquad Z\to-\infty \qquad R\geq 1 \qquad (10a)$$

$$C=1 \qquad 0\leq Z\leq 1 \qquad R=1 \qquad (10b)$$

$$\frac{\partial C}{\partial R}=0 \qquad Z<0 \vee Z>1 \qquad R=1 \qquad (10c)$$

$$C\to 0 \qquad \forall Z \qquad R\to+\infty \qquad (10d)$$

$$C\to 0 \qquad Z\to+\infty \qquad R\geq 1 \qquad (10e)$$

Equation (9) is to be solved numerically over the ranges of interest of Pe' and L/d_1 and the solution has to satisfy the boundary conditions (10a-e).

NUMERICAL METHOD

Equations (6) and (9) were solved numerically, using a finite-difference method in a non-uniform grid (Ferziger and Peric, 1996), sketched in Figure 3, similar to that adopted by Guedes de Carvalho et al. (2004). A second-order central differencing scheme was adopted for the discretisation of the diffusive terms and the convective term was discretised using the CUBISTA high-resolution scheme (see Delgado, 2006), which preserves boundedness, even for highly advective flows.

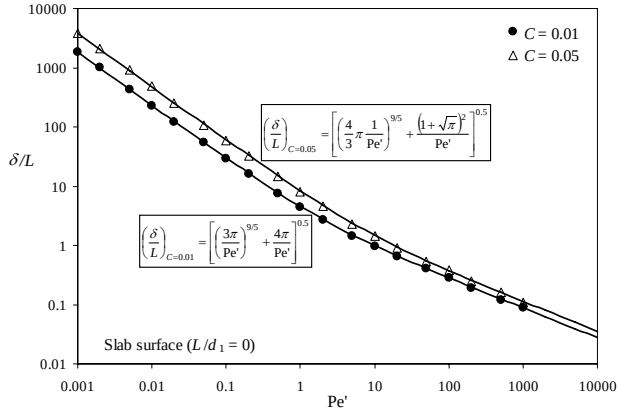

Figure 3: Dependence of δ/L on Pe' for a slab surface. The points represent the numerical solution and the solid lines correspond to Eqs. (20) an (21).

The discretised equation resulting from the finite-difference approximation of Eqs. (6) and (9), respectively, reads:

$$Pe'\frac{C_{i+1/2,j}-C_{i-1/2,j}}{(\Delta Z_i+\Delta Z_{i+1})/2}=\frac{C_{i+1,j}(\Delta Z_i)-C_{i,j}(\Delta Z_i+\Delta Z_{i+1})+C_{i-1,j}(\Delta Z_{i+1})}{\Delta Z_i\ \Delta Z_{i+1}\ (\Delta Z_i+\Delta Z_{i+1})/2}+$$

$$\frac{C_{i,j+1}(\Delta Y_j)-C_{i,j}(\Delta Y_j+\Delta Y_{j+1})+C_{i,j-1}(\Delta Y_{j+1})}{\Delta Y_j\ \Delta Y_{j+1}\ (\Delta Y_j+\Delta Y_{j+1})/2} \qquad (11a)$$

$$Pe'\frac{C_{i+1/2,j}-C_{i-1/2,j}}{(\Delta Z_i+\Delta Z_{i+1})/2}=\frac{C_{i+1,j}(\Delta Z_i)-C_{i,j}(\Delta Z_i+\Delta Z_{i+1})+C_{i-1,j}(\Delta Z_{i+1})}{\Delta Z_i\ \Delta Z_{i+1}\ (\Delta Z_i+\Delta Z_{i+1})/2}+4\left(\frac{L}{d_1}\right)^2\frac{1}{R_j}\times$$

$$\frac{(R_j+R_{j+1})\Delta R_j\ C_{i,j+1}-\left[(R_j+R_{j+1})\Delta R_j+(R_j+R_{j-1})\Delta R_{j+1}\right]C_{i,j}+(R_j+R_{j-1})\Delta R_{j+1}\ C_{i,j-1}}{\Delta R_j\ \Delta R_{j+1}\ (\Delta R_j+\Delta R_{j+1})} \qquad (11b)$$

It is important that the $C_{i+1/2,j}$ and $C_{i-1/2,j}$ values be adequately interpolated from the known grid node values using the CUBISTA high-resolution scheme to ensure numerical stability and good precision. The normalised variable approach (NVA) of Leonard (1988) was adopted, in which a general differencing scheme of order 3 or less can be expressed as:

$$C_{i+1/2,j} = f(C_{i-1,j}, C_{i,j}, C_{i+1,j}) \tag{12}$$

The NVA uses an appropriate upwind biased normalisation, and Eq. (12) can be rewritten in compact form as:

$$\hat{C}_{i+1/2,j} = f(\hat{C}_{i,j}) \tag{13}$$

where

$$\hat{C}_{k,j} = \frac{C_{k,j} - C_{i-1,j}}{C_{i+1,j} - C_{i-1,j}} \qquad (\text{for } k = i-1,\ i,\ i+1/2,\ i+1) \tag{14}$$

By definition of Eq. (14), $\hat{C}_{i-1,j} = 0$ and $\hat{C}_{i+1,j} = 1$, thus reducing Eq. (12) to a single variable or function (Eq. (13)).

The CUBISTA scheme may be represented in the context of the NVA by the following piecewise linear function:

$$\hat{C}_{i+1/2,j} = \begin{cases} \frac{7}{4}\hat{C}_{i,j} & 0 \le \hat{C}_{i,j} < \frac{3}{8} \\ \frac{3}{4}\hat{C}_{i,j} + \frac{3}{8} & \frac{3}{8} \le \hat{C}_{i,j} \le \frac{3}{4} \quad \text{QUICK} \\ \frac{1}{4}\hat{C}_{i,j} + \frac{3}{4} & \frac{3}{4} < \hat{C}_{i,j} \le 1 \\ \hat{C}_{i,j} & \text{elsewhere} \quad \text{UDS} \end{cases} \tag{15}$$

In the present work the resulting system of equations was solved iteratively by using the successive over-relaxation (SOR) method (Ferziger and Peric, 1996), and the implementation of the boundary conditions was carried out in the same way as described in our previous work (Guedes de Carvalho et al., 2004). For the situation under study, an orthogonal mesh is adequate and care was taken to ensure proper refinement in the regions where the highest concentration gradients were expected. The computational domain was varied according to the flow conditions (typically for small Pe', wider meshes were needed) and, during mesh refinement, the number of nodes along each direction was doubled and the corresponding contraction/ expansion factors were root-squared.

For all the conditions simulated in the present work, detailed mesh refinement studies were undertaken. The mesh refinement was performed in at least three meshes and continued until the difference between the calculated values of boundary layer thickness, δ/L (see Figure 1(b)), obtained in the finest mesh and the extrapolated value of δ/L (obtained using Richardson's extrapolation technique – see Eqs. (16) and (17), below) fell below 0.1%.

The values of $(\delta/L)_{ext}$ were obtained by applying Richardson's extrapolation to the limit, after determining the true order of convergence of the method, which is estimated from (Ferziger and Peric, 1996)

$$p = \frac{\log \dfrac{(\delta/L)_{medium} - (\delta/L)_{coarse}}{(\delta/L)_{fine} - (\delta/L)_{medium}}}{\log\ 2} \tag{16}$$

$$\left(\frac{\delta}{L}\right)_{ext} = \left(\frac{\delta}{L}\right)_{fine} + \frac{(\delta/L)_{fine} - (\delta/L)_{medium}}{2^p - 1} \tag{17}$$

Numerical solutions were performed within the ranges $10^{-3} \le Pe' \le 10^3$ and $0 \le L/d_1 \le 100$ which corresponds to a considerable variation of the relevant hydrodynamic and geometrical parameters. The results are shown as point values in the plots of Figures 3 to 5 and represent what may be called "the exact solution" of the problem, within the accuracy of the numerical method. For practical purposes, it is useful to have some approximate analytical expression for $\delta/L = f(Pe', L/d_1)$, which represents the exact solution with good accuracy; the development of such an expression is detailed in the following section.

RESULTS AND DISCUSSION

In this work, we defined the concentration boundary layer thickness, δ/L, as the vertical distance from the cylindrical or flat surfaces where

the solute concentration is 1% or 5% of the saturation concentration ($C = 0.01$ or $C = 0.05$, respectively).

Case I - Soluble Flat Slab

The numerical solution of Eq. (6) gives the concentration field and, from it, the concentration boundary layer thickness, δ/L, for $C = 0.01$ and $C = 0.05$.

For very low Pe'_p (say, $Pe'_p < 0.2$), dispersion is the direct result of molecular diffusion, with $D_T = D_L = D'_m$. The plot of Figure 3 reveals two well-known asymptotes, for high values of Pe':

$$\left(\frac{\delta}{L}\right)_{C=0.01} = \left[\frac{4\pi}{Pe'}\right]^{0.5} \tag{18}$$

$$\left(\frac{\delta}{L}\right)_{C=0.05} = \left[\frac{\left(1+\sqrt{\pi}\right)^2}{Pe'}\right]^{0.5} \tag{19}$$

as suggested by the analytical development of Eq. (3). Taking the asymptotes as starting guide lines, an effort was then made to obtain a general approximate expression, which would represent the "numerical points" with good accuracy over the whole range of Pe'. The function obtained were

$$\left(\frac{\delta}{L}\right)_{C=0.01} = \left[\left(\frac{3\pi}{Pe'}\right)^{9/5} + \frac{4\pi}{Pe'}\right]^{0.5} \tag{20}$$

$$\left(\frac{\delta}{L}\right)_{C=0.05} = \left[\left(\frac{4}{3}\pi\frac{1}{Pe'}\right)^{9/5} + \frac{\left(1+\sqrt{\pi}\right)^2}{Pe'}\right]^{0.5} \tag{21}$$

and the numerical values do not deviate by more than 4% from the values given by Eqs. (18) and (19), over the entire range of values of Pe'.

Case II - Cylinder Aligned with the Flow

For each value of $L/d_1 > 0.5$, the plot of δ/L vs. Pe' reveals a horizontal asymptote, for $Pe' \to 0$. This limiting value of δ/L corresponds to the situation of pure molecular diffusion, with no flow. Figures 4 show the observed dependence of $(\delta/L)_{Pe'\to 0}$ on L/d_1 and, again, two asymptotes are revealed by the plots:

$$\left(\frac{\delta}{L}\right)_{C=0.01} = \left[\left(\frac{5}{14\pi^4}\frac{L}{d_1}\right)^{-4/3} + 500\left(\frac{L}{d_1}\right)^{-1/3}\right]^{0.5} \tag{22}$$

$$\left(\frac{\delta}{L}\right)_{C=0.05} = \left[\left(\frac{3}{7\pi^2}\frac{L}{d_1}\right)^{-4/3} + 20\left(\frac{L}{d_1}\right)^{-1/3}\right]^{0.5} \tag{23}$$

Employing the above asymptotes and the asymptote for high values of Pe', an effort was made to obtain a general approximate expression for δ/L that has the correct asymptotic behaviour. The functions obtained were:

$$\left(\frac{\delta}{L}\right)_{C=0.01} = \frac{1}{\sqrt{\dfrac{1}{\left(\dfrac{5}{14\pi^4}\dfrac{L}{d_1}\right)^{-4/3} + 500\left(\dfrac{L}{d_1}\right)^{-1/3}} + \dfrac{1}{24\left(\dfrac{L}{d_1}\right)^{-2/9} Pe'^{-6/5} + \dfrac{4\pi}{Pe'}}}} \tag{24}$$

$$\left(\frac{\delta}{L}\right)_{C=0.05} = \frac{1}{\sqrt{\dfrac{1}{\left(\dfrac{3}{7\pi^2}\dfrac{L}{d_1}\right)^{-4/3} + 20\left(\dfrac{L}{d_1}\right)^{-1/3}} + \dfrac{Pe'}{\left(1+\sqrt{\pi}\right)^2}}} \tag{25}$$

and are represented in Figures 5 and 6 alongside the points obtained from the numerical solution. These do not deviate by more than 9% from the values given by Eqs. (24) and (25), over the entire range of values of Pe' and $L/d_1 \geq 0.5$.

Figures 3, 5 and 6 show that, as Pe' is reduced, the concentration boundary layer thickness increases and nonlinearity of the velocity profile becomes more important. Another important conclusion of these figures is that the asymptote for high Pe' values is $\delta/L \to Pe'^{-1/2}$. This is not surprising since, for a thin concentration boundary layer, the curvature of the cylinder is not a relevant parameter.

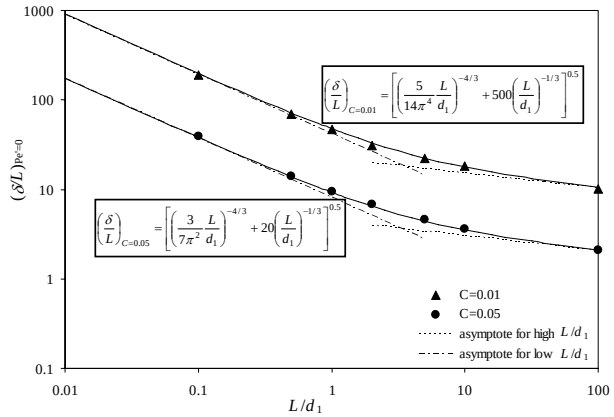

Figure 4: Dependence of $(\delta/L)_{Pe'\to 0}$ on L/d_1.

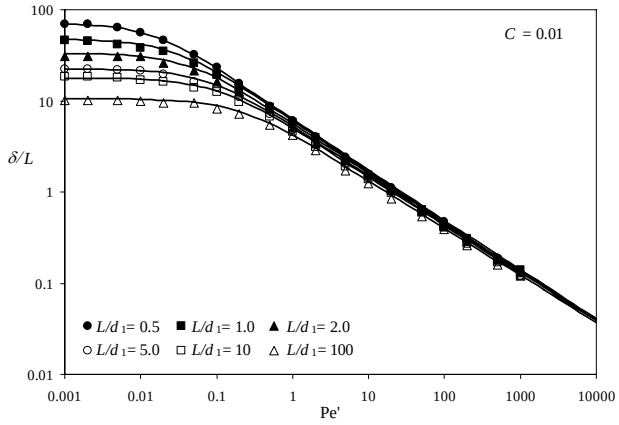

Figure 5: Dependence of δ/L on Pe' for different values of L/d_1 and $C = 0.01$. The points represent the numerical solution and the solid lines correspond to Eq. (24).

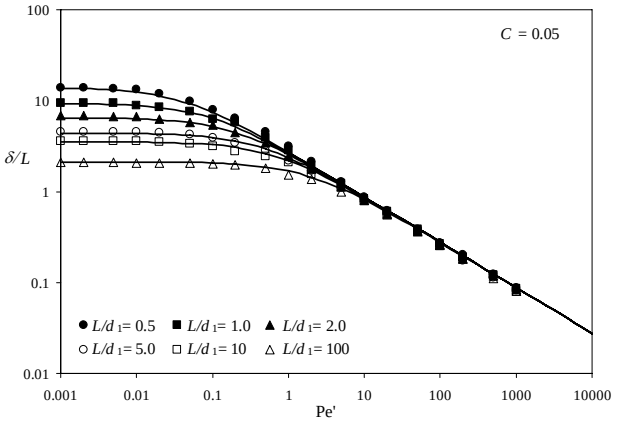

Figure 6: Dependence of δ/L on Pe' for different values of L/d_1 and $C = 0.05$. The points represent the numerical solution and the solid lines correspond to Eq. (25).

CONCLUSIONS

The problem of boundary layer development from an active cylinder and slab surface buried in a packed bed of inert particles, through which fluid flows with uniform velocity, was treated in detail.

The partial differential equations resulting from the differential mass balance were solved numerically over a wide range of values of the relevant parameters and general expressions, given as Eqs. (20), (21), (24) and (25), were obtained to relate the concentration boundary layer thickness with the Peclet number and the ratio between length and diameter of the soluble cylinder.

The theory developed applies only in the range $ud/D'_m < 0.2$, over which dispersion is the result of only advection and molecular diffusion.

ACKNOWLEDGMENT

The author wishes to thank the Fundação para a Ciência e a Tecnologia for the Grant Nº SFRH/BPD/11639/2002.

NOMENCALTURE

a	Radius of soluble cylinder
c	Solute concentration
c_0	Bulk concentration of solute
c^*	Equilibrium concentration of solute
C	Dimensionless solute concentration
d	Diameter of inert particles

d_1	Diameter of soluble cylinder
D_L	Longitudinal dispersion coefficient
D_m	Molecular diffusion coefficient
D'_m	Effective molecular diffusion coefficient ($= D_m / \tau$)
D_T	Transverse dispersion coefficient
L	Length of solid slab or cylinder
p	Order of convergence
Pe'	Peclet number based on length of flat slab or cylinder ($= uL / D'_m$)
Pe'_p	Peclet number based on diameter of inert particles ($= ud / D'_m$)
R	Dimensionless spherical radial co-ordinate ($= r / a$)
r	Spherical radial coordinate
u	Absolute value of superficial velocity
y	Cartesian co-ordinate
Y	Dimensionless axial co-ordinate ($= y / L$)
z	Cartesian co-ordinate
Z	Dimensionless axial co-ordinate ($= z / L$)

Greek Letters

δ	Concentration boundary layer thickness
ε	Bed voidage
τ	Tortuosity of the packed bed

Subscripts and Superscripts

i, j	Grid node indices (see Figure 3)
n	Iteration number
ext	Extrapolated value

REFERENCES

Cheng, C. Y., Double diffusion from a vertical wavy surface in a porous medium saturated with a non-Newtonian fluid, International Communications in Heat and Mass Transfer, 34, 285 (2007).

Chrysikopoulos, C. V., Hsuan, P.-Y., Fyrillas, M. M. and Lee, K. Y., Mass transfer coefficient and concentration boundary layer thickness for a dissolving NAPL pool in porous media, Journal of Hazard. Materials, B97, 245 (2003).

Coelho, M. A. N. and Guedes de Carvalho, J. R. F., Transverse dispersion in granular beds: Part I-Mass transfer from a wall and the dispersion coefficient in packed beds, Chemical Engineering Research and Design, 66, 165 (1988).

Delgado, J. M. P. Q., Mass transfer and dispersion around an active cylinder in cross flow and buried in a packed bed, Heat Mass Transfer, 42, 1119 (2006).

Ferziger, J. H. and Peric, M., Computational methods for fluid dynamics, Berlin, Springer-Verlag (1996).

Guedes de Carvalho, J. R. F., Delgado, J. M. P. Q. and Alves, M. A., Mass transfer between flowing fluid and sphere buried in a packed bed of inerts, AIChE Journal, 50, 65 (2004).

Leonard, B. P., Simple high-accuracy resolution program for convective modelling of discontinuities, International Journal for Numerical Methods in Fluids, 8, 1291 (1988).

Nebbali, R. and Bouhadef, K., Numerical study of forced convection in a 3D flow of a non-Newtonian fluid through a porous duct, International Journal of Numerical Methods for Heat & Fluid Flow, 16, 870 (2006).

Prandtl, L., Eine beziehung zwishen wärmeaustausch und strömungwiderstand der flüssigkeiten, Physikalische Zeitschrift, 11, 1072 (1910).

Schlichting, H., Boundary layer theory, Seventh ed., McGraw-Hill, New York (1979).

Vortmeyer, D. and Schuster, J., Evaluation of steady flow profiles in rectangular and circular packed beds by a variational method, Chemical Engineering Science, 38, 1691 (1963).